RSC Advances

ROYAL SOCIETY OF CHEMISTRY

www.rsc.org/advances

ROYAL SOCIETY OF CHEMISTRY

ARTICLE

Dual-responsive star-shaped polypeptides for drug delivery

Wenlong Wang, [#a] Liang Zhang, [#a] Mengtao Liu,[a] Yuan Le,[*a] Shanshan Lv[a] and Jian-Feng Chen[ab]

Received 00th January 20xx,
Accepted 00th January 20xx

DOI: 10.1039/x0xx00000x

www.rsc.org/

Core cross-linked star shaped polypeptides based on poly(L-glutamicacid)-poly(L-phenylalanine-co-L-cystine) copolymer have been successfully synthesized and thoroughly characterized. The star polypeptides can self-assemble to form 50 nm micelles in aqueous medium, which respond rapidly to both pH change within the physiologically relevant pH range and a reduction environment mimicking the intracellular space. Water-soluble doxorubicin hydrochloride and hydrophobic resveratrol are loaded into the star polypeptides micelles through electrostatic and hydrophobic interaction respectively. The drug loading content can be controlled by tuning the composition of the star polypeptides. The *in vitro* release studies indicate dual sensitivity enabled rapid drug release at pH 5.5 and dithiothreitol (DTT) 10 mM mimic to intracellular environment. Furthermore, the star polypeptides are biocompatible and interact well with cells in vitro. Confocal fluorescence microscopy and flow cytometry assay show these star polypepides can be quickly internalized and effectively deliver the drugs into HeLa cells to inhibit cell growth.

1. Introduction

Biodegradable polymeric micelles formed by amphiphilic block copolymers have been constituting a growing interest in the fields of drug delivery,[1-3] owing to their excellent performance in enhancing drug solubility, prolonging drug circulation time and minimizing side effects.[4] Various intelligent polymers in response to internal or external stimuli, such as temperature,[5] pH,[6,7] light,[8] ultrasound,[9] and redox potential,[10] have been used extensively by drug delivery systems. Among the stimulus-responsive polymers, pH and redox-responsive polymers appeared to be the most attractive candidate for targeted and controlled drug delivery because of the significant differences in the glutathione (GSH) concentration and pH between different physiological tissue.[11,12] The physiological pH of blood and normal tissues is 7.4, but the extracellular pH in some tumor tissues is 6.8, and the intracellular endo/lysosomal pH ranges from 4.0 to 5.5.[13,14] Meanwhile, the GSH concentration is 2-20 μM in blood and normal tissue, but it is around 10 mM in tumor cells. [15] Thus, these dual-stimuli responsive polymers have unprecedented control over drug release and delivery to increase efficacy *in vitro* and in vivo.[16-18]

Although much research has been carried out on polymeric micelles for stimuli-responsive drug delivery systems, their clinical applications are facing tremendous challenges including poor *in vivo* stability, low drug loading levels and slow drug release.[19,20] In comparison with conventional linear polymers, star polymers with three-dimensional architecture exhibit unique properties such as enhanced stability,[21] high encapsulation capabilities,[22] as well as large number of internal and peripheral functionalities.[23,24] They are expected for potential clinic application. Polypeptides, which are poly(amino acid)s linked by peptide bonds, are unique biodegradable and biocompatible polymers with structures mimicking natural proteins.[25] Meanwhile, polypeptides can offer transitions in response to external stimuli,[26,27] and their side chains could be incorporated with various functional moieties for designing intelligent polymer systems.[28-30] Therefore, it is interesting to explore the potential of stimul-responsive star polypeptide for improving drug delivery.

To our knowledge, star polypeptides as dual pH and redox-responsive micelles have not been reported yet. Moreover, the reported responsive polymers carry drugs just through physical interaction or via chemical conjugation despite that both hydrophilic and hydrophobic drugs can be entrapped into the polymeric micelles.[31-33] In addition, the process of encapsulation, tunable parameters, and biocompatibility are not well characterized for the application of drug delivery. There is great demand to design smart system with enhanced functionality and precise molecular control.

[a] *State Key Laboratory of Organic-Inorganic Composites, Beijing University of Chemical Technology, Beijing 100029, P.R. China*
[b] *Research Center of the Ministry of Education for High gravity Engineering and Technology, Beijing University of Chemical Technology, Beijing 100029, PR China*
# These authors contributed equally to this work.

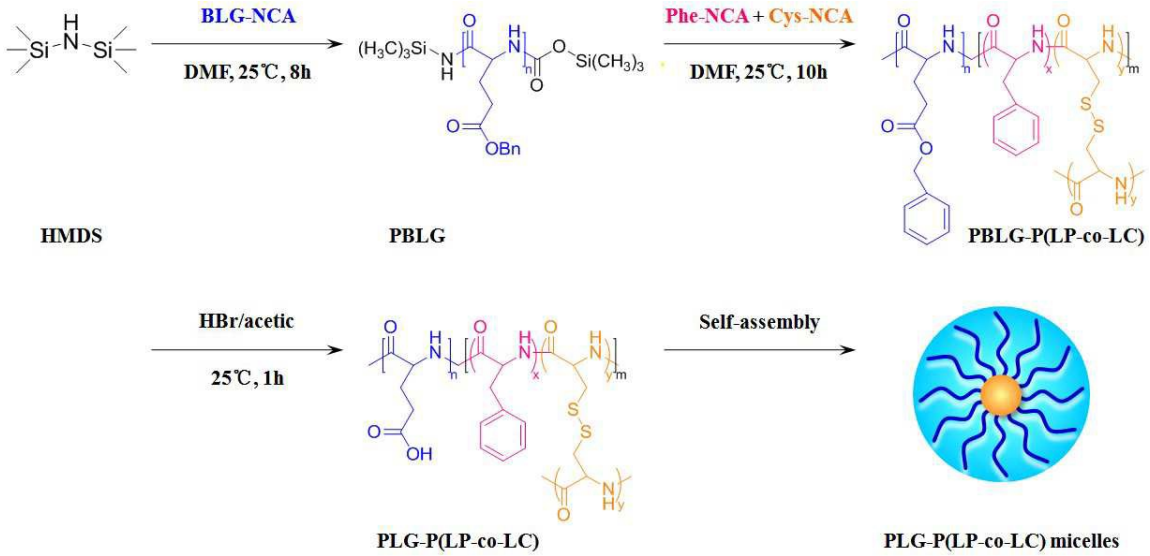

Scheme 1. Synthetic strategy toward star polypeptides PLG-P(LP-co-LC).

In this work, we designed a novel core cross-linked star polypeptides based on poly(L-glutamic acid)-poly(L-phenylalanine-co-L-cystine) (PLG-P(LP-co-LC)) for dual responsive drug delivery, as shown in scheme 1. By taking advantages of the star polypeptides properties, PLG-P(LP-co-LC) copolymers are expected to undergo spontaneous self-assembling to micelles in the aqueous solutions resulting in the PLG outer corona and hydrophobic PLP/PLC inner core. Doxorubicin hydrochloride (DOX) was selected as a hydrophilic drug and resveratrol (RES) was used as a hydrophobic drug. RES (trans-3, 5, 4'-trihydroxy-stilbene), a natural polyphenol compound found in grapes and berries,[34,35] is well-known for its activities of antioxidant, cardioprotect, anti-inflammatory[36] as well as anti-cancers.[37,38] The anionic PLG provides the strong electrostatic interaction with cationic DOX, and the hydrophobic PLP serves as a reservoir for RES. The physiochemical properties, drug loading and release performances of the star polypeptides have been investigated. Furthermore, cell cytotoxicity and internalization behavior of the drug loaded star polypeptides have also been explored to evaluate the potential for in vivo drug delivery.

2. Experimental

2.1 Materials

L-glutamic acid, L-phenylalanine, L-cystine, dithiothreitol (DTT), doxorubicin hydrochloride (DOX) and resveratrol (RES) were purchased from Aladdin Industrial Corporation(Shanghai, China). Benzyl-L-glutamate (BLG) and N-Benzyloxycarbonyl -L-cystine (Z-L-cystine) were synthesized according to the literature procedure.[39,40] Hexamethyldisilazane (HMDS) (99.9%), anhydrous N,N-dimethylformamide (DMF), 3-(4,5-dimethylthiazol-2-yl)-2,5-diphenyltetrazolium bromide (MTT), and 4',6-diamidino-2-phenylindole dihydrochloride (DAPI) were purchased from Sigma-Aldrich (St Louis, MO, USA) and used as received. Tetrahydrofuran (THF), dichloromethane (DCM), 1,4-dioxane were obtained from Sinopharm Chemical Reagent (Beijing, China) and distilled prior to use. All the other reagents and solvents were analytical grade and used without further purification.

2.2 Characterizations

NMR spectroscopy was performed on Bruker AV Ⅲ 400 NMR spectrometer using the deuterated solvent as reference and a sample concentration of ca. 20 mgmL^{-1}. FT-IR spectra was recorded on Bruker VERTEX 70 instrument using the potassium bromide (KBr) method. The carbon, hydrogen, nitrogen and sulfur element contents of star polypeptides were estimated by Vaio EL cube elemental analysis. Scanning electron microscopy (SEM) measurement was performed on JEOL JSM-7800F at an accelerating voltage of 10 KV. A drop of the micelles solution (0.05 gL^{-1}) was deposited onto a piece of cover glass and allowed to dry in air at 25 ℃ before measurements. Dynamic laser scattering (DLS) measurements were performed on Malvern ZS90 with a vertically polarized He-Ne laser (633 nm) at an angle of 173° and a temperature of 25 ± 0.1 ℃. The initial PBLG or PBLG-P(LP-co-LC) concentrations of 10 mgmL^{-1} in DMF were used then serial dilutions were performed until stable spectra were obtained. All sample solutions were filtered using 0.45 μm filters. Molecular weight and molecular weight distributions were determined using Agilent 2600 Series Gel penetration chromatograph (GPC) instrument at 25 ℃ using DMF with 0.5 M LiBr as the eluent at a flow rate of 1 mL min^{-1}. The standard curve was determined using a series of narrow distribution polystyrene standard samples.

2.3 Synthesis of BLG-NCA, Phe-NCA and Cys-NCA

The amino acids were converted to their NCA derivatives using either triphosgene or thionyl chloride, respectively. Benzyl-L-glutamate (1.8 g, 7.6 mmol) was dissolved in 30 mL THF under nitrogen. Triphosgene (0.9 g, 2.9 mmol) was added and the mixture was stirred at 40 ℃ until the cloudy solution turned clear. The solvent was removed in vacuo and the resulting residue was purified by recrystallization with ethyl acetate and n-hexane to afford γ-Benzyl-L-glutamate-N-carboxyanhydride (BLG-NCA) (yield: 95.1%). ^{1}H NMR (400 MHz, $CDCl_3$, δ_H, ppm): 2.21 (m, 2H, -CH_2-), 2.60 (dd, 2H, -CH_2COO), 4.45 (t, 1H, -CHN-), 5.15 (s, 2H, -CH_2O), 7.35 (m, 5H, ArH-), 6.28 (s, 1H, -NH-). L-phenylalanine N-carboxyanhydride (Phe-NCA) was synthesized following the same procedure as the synthesis of the BLG-NCA (yield: 91.5%). ^{1}H NMR (400 MHz, $CDCl_3$, δ_H, ppm): 3.15 (m, 2H, -CH_2-), 4.53 (dd, 2H, -CHN-), 5.78 (s, 1H, -NH-), 7.30 (m, 5H, ArH-).

Z-L-cystine (2.0 g, 3.9 mmol) was dissolved in 20 mL 1,4-dioxane. Thionyl chloride (1.2 mL, 16.5 mmol) was added and the mixture was reacted at 55 ℃ for 3h. After removal of the solvent in vacuo, the resulting residue was precipitated in DCM to obtain L-cystine N-carboxyanhydride (Cys-NCA) (yield: 92.3%). ^{1}H NMR (400 MHz, DMSO-d_6, δ_H, ppm) 3.20 (m, 4H, -SCH_2CH-), 4.77 (dd, 2H, -CHN-), 9.25 (s, 2H, -NH-).

2.4 Synthesis of star polypeptides PLG-P(LP-co-LC)

The star polypeptides PLG-P(LP-co-LC) were synthesized through one-step ring-opening polymerization of BLG-NCA, Cys-NCA and Phe-NCA in DMF using HMDS as the initiator. In brief, BLG-NCA (1.0 g, 3.3 mmol) and HMDS (17 μL, 82 μmol) was dissolved in anhydrous DMF (10 mL) in a glove box. The reaction mixture was stirred at room temperature until the NCA's anhydride peak at 1786 cm^{-1} disappeared, as determined by FT-IR. After diluting the concentration of poly(γ-benzyl-L-glutamate) (PBLG) to 1 $mgmL^{-1}$ using DMF (containing 0.1 M LiBr) for measuring the molecular weight of PBLG. Then, Phe-NCA (0.4 g, 2.3 mmol) and Cys-NCA (0.3 g, 1.0 mmol) were added to the remaining PBLG solution, and the reaction was maintained for another 10 h. The polymer solution was precipitated into excess amount of methanol to afford the resulting star polypeptides PBLG-P(LP-co- LC) (yield: 86.5%). ^{1}H NMR (400 MHz, TFA-d_6, δ_H, ppm): 2.21 (d, 2H, -$CHCH_2$-), 2.48 (s, 2H, -CH_2COOH), 4.80 (s, 2H, $CH_2C_6H_5$), 5.33 (s, H, -CHN), 7.78 (m, 5H, ArH-).

Subsequently, star polypeptides PBLG-P(LP-co-LC) (2.0 g) were dissolved in TFA (10 mL) and 4 mL HBr (33% in acetic acid) was added. After stirring for 1 h at room temperature, the mixture was precipitated into excess amount of ice diethyl ether. After dried under vacuum, the crude product was purified by dialysis against deionized water (MWCO=3500 Da), and lyophilized to afford water soluble star polypeptides PLG-P(LP-co-LC), yielding a white solid (yield: 87.2%). ^{1}H NMR (400 MHz, D_2O, δ_H, ppm): 1.92 (d, 2H, -$CHCH_2$-), 2.23 (s, 2H, -CH_2COOH), 4.26 (s, H, -CHN-), 7.26 (m, 5H, ArH-).

2.5 Stimuli Responsive of star polypeptides

The blank micelles were prepared by dialysis method. The star polypeptides PLG-P(LP-co-LC) were dissolved in dimethyl sulfoxide (DMSO), and the solution was added to deionized water under stirring for 24 h. To remove the solvents, the solution was dialyzed against deionized water for 72 h.

The pH-responsibility of PLG-P(LP-co-LC) was examined by analyzing the size and zeta potential of the micelles solution at different pH values using DLS. Furthermore, the disassembly of micelles in response to redox stimuli was examined by DLS and ^{1}H NMR spectroscopy. DTT was dissolved in degassed micelles solution (10 mM DTT) under nitrogen. The obtained solution was stirred at 37 ℃, and the size of PLG-P(LP-co-LC) was determined by DLS at different time intervals. After 24 h, the resulting solution was dialyzed and lyophilized for ^{1}H NMR analysis.

2.6 Preparation of drug loaded micelles

The DOX-loaded micelles were prepared according to the following method. In brief, PLG-P(LP-co-LC) (50 mg) was dissolved in distilled water and DOX (10 mg) dissolved in DMSO was added dropwise. After stirring overnight in the dark, the organic solvent and free DOX were removed by dialysis using a dialysis bag (MWCO=3500 Da) against deionized water for 24 h, and then freeze-dried to obtain the DOX-loaded micelles.

The RES-loaded micelles were prepared by a dialysis method. Briefly, 50 mg of PLG-P(LP-co-LC) and 5 mg of RES were dissolved in DMSO, and the solution was added dropwise to the deionized water under stirring. The mixture was maintained at room temperature under stirring for 12 h. The solution was dialyzed against excess deionized water with a dialysis bag (MWCO=3500 Da) for 24 h, and then filtered through a 0.45 μm pore-sized microporous membrane. The RES-loaded micelles were obtained after lyophilization.

DOX loaded micelles were determined by UV absorption at 480 nm and RES loaded micelles were detected at 306 nm. The drug loading content (DLC, wt%) and drug loading efficiency (DLE, wt%) were calculated according to the following formulas

$$\mathrm{DLC} = \left(\frac{\text{amount of loaded drug}}{\text{amount of drug - loaded micelles}} \right) \times 100\%$$

$$\mathrm{DLE} = \left(\frac{\text{amount of loaded drug}}{\text{amount of feeding drug}} \right) \times 100\%$$

2.7 *In vitro* drug release

The release profiles of drugs from micelles were investigated in PBS at different pH values (7.4, 6.8 and 5.5) or different concentrations of DTT (0 mM, 5 mM and 10 mM) by the dialysis method. The weighed freeze-dried drug loaded micelles were suspended in 5 mL of the release medium and transferred into a dialysis bag (MWCO=3500 Da). The release experiment was initiated by placing the dialysis bag into release medium at 37 ℃ with continuous shaking at 100 rpm. At predetermined intervals, 5 mL of the incubated solution was withdrawn and replaced with equal volume of fresh release medium. The amounts of DOX and RES were determined using UV-Vis spectrometer (SHIMADZU UV 2600)

at 480 nm and 306 nm, respectively. All measurements were conducted in triplicate.

2.8 Cell cultures

HeLa cells were cultured in Dulbecco's modified Eagle's medium (DMEM) containing 10% fetal bovine serum (FBS), Supplemented with 50U mL^{-1} penicillin and 50U mL^{-1} streptomycin, and incubated at 37 ℃ in 5% CO_2 atmosphere.

2.9 Cell viability assays

The *in vitro* cytotoxicities of blank micelles, free drugs, and drug loaded micelles were assessed with MTT assays. HeLa cells were seeded in 96-well plates at ~4000 cells per well in 100 μL of DMEM containing 10% fetal bovine serum, supplemented with 50U mL^{-1} penicillin and 50U mL^{-1} streptomycin, and incubated at 37 ℃ in 5% CO_2 atmosphere for 24 h. The culture mediums were replaced with 200 μL fresh mediums containing different concentrations of star polypeptides (0~500 μgmL^{-1}). The absorbency of the solution was measured on Multiskan MK3 microplate reader at 490 nm. The cell viability (%) was calculated by $(A_{sample}/A_{control}) \times 100$, where A_{sample} and $A_{control}$ denoted as the absorbencies of the sample and control wells, respectively. Data are presented as means ± standard deviation (n = 3).

2.10 Intracellular drug release

The cellular uptake and intracellular release behaviors of DOX loaded micelles were determined by confocal laser scanning microscopy (CLSM) toward HeLa cells. The cells were seeded on coverslips in 6-well plates with a density of ~40 000 cells per well in 2 mL of DMEM and cultured for 24 h, and the cells were incubated with DOX loaded micelles at a concentration of 20 μgmL^{-1} in complete DMEM. After 4 h, 12 h and 24 h incubation, the culture medium was removed and cells were washed three times with PBS. Then, the cells were fixed with 4% paraformaldehyde at room temperature, and the cell nuclei were stained with 4', 6-diamidino-2-phenylindole (DAPI). The treated cells were visualized under a laser scanning confocal microscope (Leica TCS SP5).

The cellular uptake of micelles was also analyzed quantitatively using flow cytometry. HeLa cells were seeded at a density of 2×10^4 cells per well in 6-well plates and incubated for 24 h. After incubating with DOX loaded micelles (at a concentration of 20 μgmL^{-1}) for 4, 12 and 24 h, the cells were washed three times with PBS, harvested and subsequently resuspended in 0.5 mL PBS for flow cytometry analysis (FC500, Beckman Coulter, USA). The instrument was calibrated with non-treated cells (negative control) to identify viable cells, and the cells were determined from a fluorescence scan performed with 1×10^4 cells using the FL1-H channel.

2.11 Statistical analysis

All the values were presented as mean ± standard deviation (SD) of at least three independent measurement. Statistical significance was tested by one-way ANOVA followed by a Student's t-test for multiple comparison tests. Difference characterized by *P < 0.05 were considered statistically signify-cant. All statistical analysis was performed using SPSS, version 22.

3. Results and discussion

3.1 Synthesis and characterization of star polypeptides PLG-P(LP-co-LC)

The star polypeptides PLG-P(LP-co-LC) were synthesized through core cross-linked strategy using sequential ring opening polymerization of BLG-NCA, Phe-NCA and Cys-NCA using HMDS as initiator, followed by deprotecting the groups in HBr/acetic acid. The structures of NCA monomers were Identified by FT-IR and ^{1}H NMR. Fig. 1S showed the FT-IR spectra of NCA monomers with various amino acid. The peaks centered at 1750 and 1850 cm^{-1} were assigned to characteristic peak of carbonyl from anhydride. As shown in Fig. 2SA, the resonances at 7.35 ppm (peak a) and 6.28 ppm (peak d) were ascribed to the Ar of BLG and NH of NCA. In Fig. 2SB, the peaks at 4.53 ppm (peak c) and 5.78 ppm (peak b) were assigned to the CH and NH of anhydride. Peaks a indicated the presence of benzene in Phe-NCA. Fig. 2SC showed that the peaks at 9.25 ppm and 3.20 ppm were ascribed to NH and CH_2 of Cys-NCA. The ^{1}H NMR and FT-IR spectroscopy confirmed the successful synthesis of NCA monomers.

Then, the polymerization initiated by HMDS was monitored via FT-IR intensity of NCA's anhydride peak at 1787 cm^{-1},[41,42] the disappearance of NCA's anhydride peak confirmed the complete consumption of the monomers. Upon addition of Phe-NCA and cross-linker Cys-NCA, the weight average molar mass(Mw) of polypeptides increased from 7.5 kDa to 932.4 kDa (Fig. 1A), and the size measured by DLS significantly increased from 8.5 nm to 101.3 nm (Fig. 1B). The ^{1}H NMR spectrum of PBLG-P(LP-co-LC) (Fig. 2B) showed the characteristic signals (peak a) in BLG units, but the signals of the cross-linked core component were not visible due to the

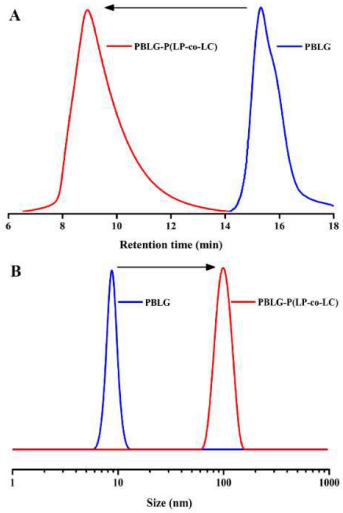

Fig. 1 GPC RI chromatograms (A) and size (B) of PBLG and PBLG-P(LP-co-LC) in DMF.

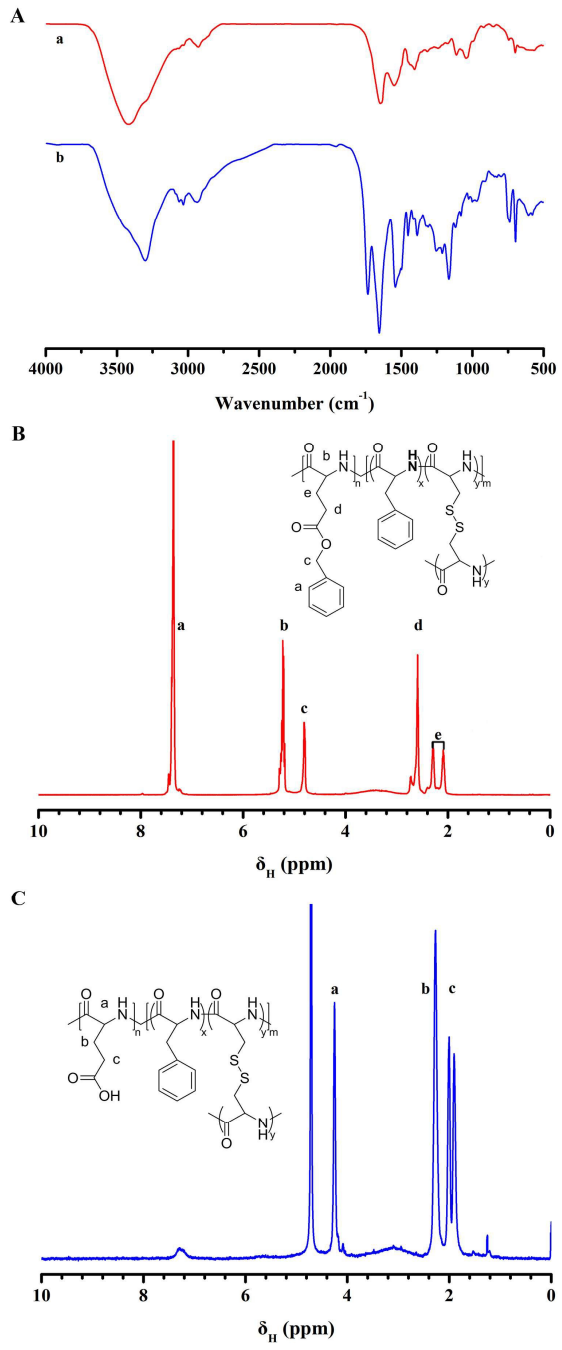

Fig. 2 FT-IR spectra (A) of star polypeptides PLG-P(LP-co-LC) (a) and PBLG–P (LP-co-LC) (b); ^{1}H NMR of PBLG-P(LP-co-LC) (B, TFA-d_6) and PLG-P(LP-co-LC) (C, D_2O).

reduced segmental mobility.[43,44] Furthermore, PLG-P(LP-co-LC) was prepared by removing the benzylox-ycarbonyl groups of PBLG-P(LP-co-LC). The disappearrance of the ester C=O stretching peak at 1725 cm^{-1} (Fig. 2A) and the benzyl group signal at 7.36 ppm (Fig. 2C) indicated the complete removing of the protective group in the polypeptides. The final molar composition ratio of the monomeric repeating units in PLG, PLP and PLC blocks was 40:24:10 (calculated by elemental analysis).

3.2 Stimuli Responsive of Star polypeptides

The pH and redox-responsive behaviors of the star polypeptides PLG-P(LP- co-LC) were investigated by DLS and ^{1}H NMR, as shown in Fig. 3 and Fig. 4. The zeta potentials of PLG-P(LP-co-LC) significantly increased as the pH decreased, and the carboxyl groups in PLG were in a fully deionized state below pH 5.0, resulting in significant agglomeration.[45] Similar pH-dependent agglomeration was also proved by the size (Fig. 3), which dramatically increased to 1306 nm with the decrease of pH from 8 to 3. It is well known that the disulfide linkages are stable under normal physiological conditions but respond to reductive conditions (e.g. GSH, DTT) via reversible cleavage into free thiols. The star polypeptides PLG-P(LP- co-LC) could preserve their core-shell structures without DTT. In the presence of DTT (10mM), significant change of size was observed, wherein the size gradually increased from 80 to 140 nm in 5 h and over 290 nm in 24 h (Fig. 4A). These results suggest that the disulfide linkages of PLG-P(LP-co-LC) were cleaved by 10 mM DTT so that the core structure of star polypetides micelles dissociated that lead to the size increase. Meanwhile, the characteristic signals corresponding to the core segments were also observed in ^{1}H NMR spectra after cleavage, including signals at 7.2 ppm (C_6H_5- in PLP) and 2.9-3.2 ppm (-CH_2- in PLC) (Fig. 4B).

3.3 characterization of drug loaded micelles

The star polypeptides PLG-P(LP-co-LC) with hydrophilic PLG arms and hydrophobic PLP core spontaneously formed core-shell micelles in aqueous solutions. The morphologies of the micelles were studied by SEM (Fig. 5A), which showed that micelles were spherical shaped with an average diameter of around 50 nm. In contrast, the size measured by DLS were 80 nm (Fig. 5D). The smaller values from SEM observations should be due to the dehydration of the micelles during the SEM sample preparation process. Furthermore, DOX and RES were loaded into the micelles by nanoprecipitation technique. Compared to blank micelles, the size of drug loaded micelles

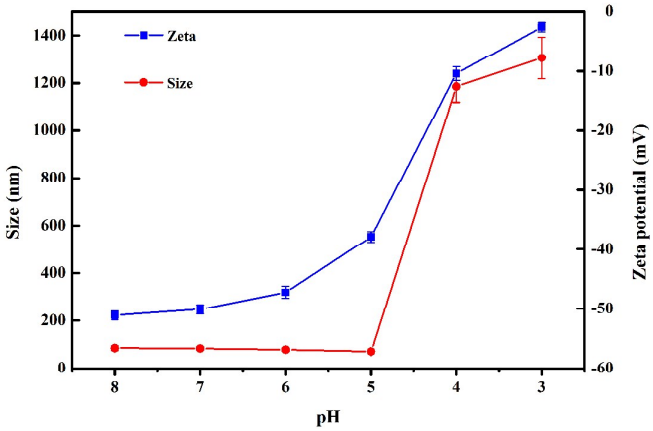

Fig. 3 Size and zeta potential of star polypeptides PLG-P(LP-co-LC) at different pH.

Table 1 Characterizations of the drug loaded micelles

Star Polypeptides	Feed ratio[a]	Resultant ratio[b]	DLC (%)		DLE (%)	
			DOX	RES	DOX	RES
PLG-P(LP-co-LC)-1	1.0 / 0.7	1.0 / 0.6	15.8	5.8	89.7	28.5
PLG-P(LP-co-LC)-2	1.0 / 1.0	1.0 / 0.8	13.2	6.9	81.6	34.3
PLG-P(LP-co-LC)-3	1.0 / 1.2	1.0 / 1.0	7.8	10.1	65.3	50.5

[a]Feed molar ratio of BLG NCA/Phe NCA.

[b]Resultant molar ratio of PLG /PLP calculated by elemental analysis.

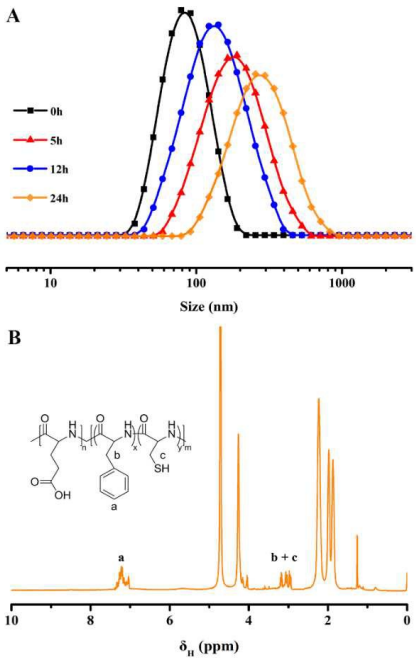

Fig. 4 Size (A) and ^{1}H NMR spectra (B, D_2O) of star polypeptides PLG-P(LP-co-LC) response to 10 mM DTT.

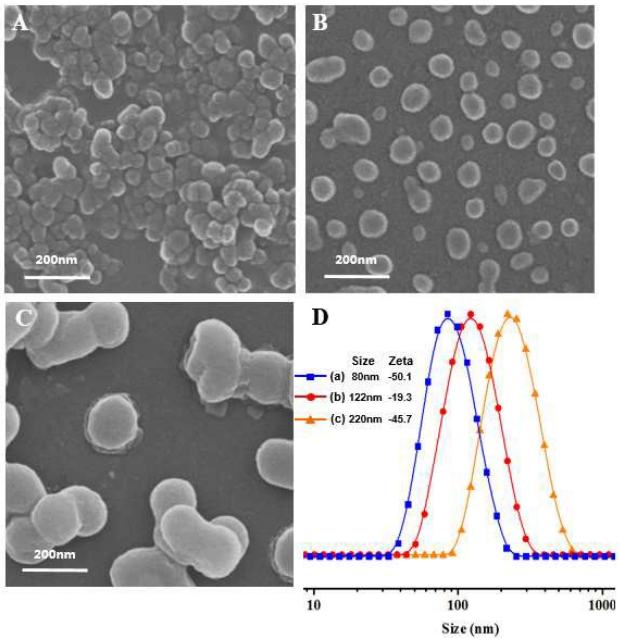

Fig. 5 SEM micrographs of blank micelles (A), DOX loaded micelles (B) and RES loaded micelles (C); Size and zeta potentials (D) of blank micelles (a), DOX loaded micelles (b) and RES loaded micelles (c).

increased and maintained a narrow distribution as shown in Fig. 5D, which confirmed drugs being effectively entrapped into micelles. Meanwhile, the morphologies of the drug loaded micelles were measured by SEM measurement. SEM images revealed that all micelles possessed uniformly spherical morphologies.

Then, drug loading capacity (DLC) and efficiency (DLE) were measured and shown in Table 1. The DLC and DLE values of DOX were higher than that of RES owing to different interactions between drugs and micelles. After DOX loading, the zeta potentials of micelles changed from -50.1 mV to -19.3 mV due to the carboxyl groups neutralized, suggesting that the positively charged DOX was captured by the carboxyl groups of PLG through electrostatic attraction.[47,48] However, RES was loaded into micelles through aromatic stacking interaction with PLP, and the zeta potentials of RES-loaded micelles displayed a slight change. In order to prove the hypothesis, we adjusted compositions of the polypeptides and investigated the DLC and DLE of both drugs (Table 1). With the ratio of hydrophilic PLG decreasing, the DLC of DOX reduced from 15.8% to 7.8% and DLE decreased to 65.3%, which was attributed to the weakened electrostatic attraction between DOX and PLG. In contrast, with the ratio of PLP increasing, hydrophobic interaction between RES and the core was enhanced, leading to an increase in the DLC and DLE of RES to 10.1%and 50.5%, respectively.[49]

3.4 Release behavior of drug loaded micelles

The DOX and RES release behaviors of micelles were assessed using a dialysis method at 37 ℃ in phosphate buffered saline (PBS) at different pH values (7.4, 6.8 and 5.5) and different concentrations of DTT (0 mM, 5 mM and 10 mM). As shown in

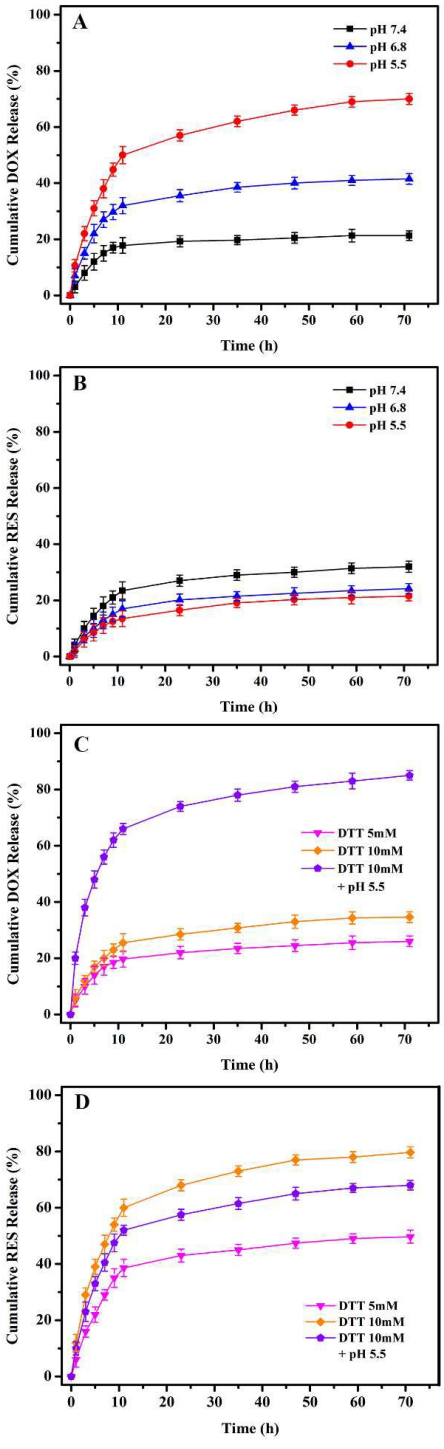

Fig. 6 *In vitro* DOX (A, C) and RES (B, D) release in PBS at 37 ℃.

Fig. 6, the release of encapsulated drugs through a change in pH have been exploited. The release of DOX was greatly influenced by the environmental acidity, about 22% and 71% of DOX were released at pH 7.4 and pH 5.5 after 72 h (Fig. 6A). However, the release of RES performed an opposite trend (Fig. 6B), with only 20% of RES released at pH 5.5 after 72 h. This pH dependent release behavior was attributed to the deionized carboxyl groups, which resulted in weakened electrostatic interaction and strengthened hydrophobic interaction.

Meanwhile, the drug release behaviors under reductive conditions were also investigated. RES release was accelerated in PBS with 10 mM DTT (Fig. 6D), about 80% of RES was released in 72 h due to the swelling of the micelles caused by the cleavage of the disulfide bonds. In comparison, the stable electrostatic interaction between the drug and the micelles resulted in only a slight increase in DOX release (Fig. 6C). Furthermore, both drugs rapidly released under simulated endosomal condition (PBS buffer at pH 5.5 with 10 mM DTT), especially in the first 10 h. Within 72 h, over 85% DOX and 72% RES were released. These results indicated that the pH and redox-sensitive stars could effectively release loaded drugs in endosomal environments.

3.5 In vitro cytotoxicity studies

The cytotoxicity of the star polypeptides PLG-P(LP-co-LC) was evaluated using MTT assay. HeLa cell lines were utilized. As shown in Fig.7, the viabilities of HeLa were ~100% at 30 μgmL^{-1} for 24 h, gradually decreased with increased concentration of polymer and incubated time. However, the viabilities of HeLa were above 80% at all test concentrations up to 500 μgmL^{-1}, revealing remarkable safety and biocompatibility of the stars PLG-P(LP-co-LC).

To verify the effect of drug-loaded system, the proliferation inhibition effects of free drugs and drug loaded micelles against HeLa cells were tested using MTT assay. The cell viability histograms were shown in Fig. 8. After 24 h, 48 h, and 72 h incubation, all free drugs and drug loaded micelles showed dose and time-dependent cell proliferation inhibition behavior. The cell viabilities incubated with free DOX and DOX-loaded micelles had similar change trends. With the increase of drug concentration from 0.6 to 10 μgmL^{-1}, cell viabilities decreased from 80% to 30% for 24 h. As the extension of cultivation time, the drugs were taken more into cells thus result in the decrease of cell viabilities. For RES, cell toxicity was lower than DOX. The IC_{50} values of free drugs and drug-loaded micelles were summarized in Table 2. The IC_{50} values of DOX loaded micelles were 2.05, 1.26 and 0.84 μgmL^{-1} for 24, 48 and 72 h, respectively, which were similar to that of free DOX. The IC_{50} values of RES loaded micelles were less than that of free RES.

Table 2 IC_{50} (μgmL^{-1}) of free drug and the drug loaded micelles.

	Free DOX	Free RES	DOX loaded micelles	RES loaded micelles
24h	2.05	33.34	2.20	22.81
48h	1.26	27.31	1.32	17.13
72h	0.84	20.08	0.89	11.40

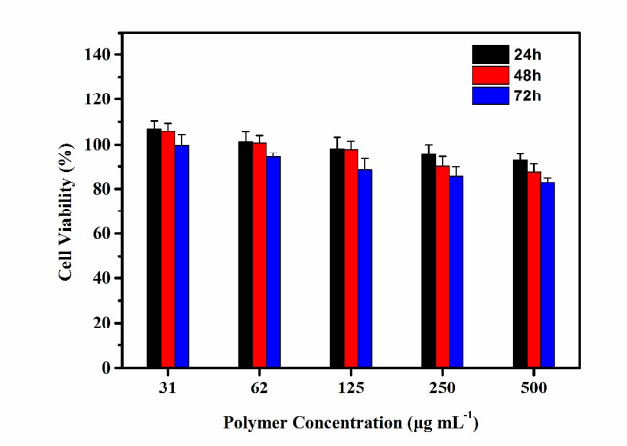

Fig. 7 Cell viabilities of HeLa incubated with PLG-P(LP- co-LC) for 24 h, 48 h and 72 h (n = 3, mean ± SD).

3.6 Cellular uptake behavior of DOX loaded micelles

The cellular uptake and intracellular release behavior of drug loaded micelles in HeLa cells were investigated by CLSM and flow cytometry. The cellular nuclei were stained with DAPI (blue). DOX (red) was loaded in PLG-P(LP-co-LC) for subcellular observation. As shown in Fig. 9A, DOX fluorescence could be observed in the cell cytoplasm and distributed widely in the cytoplasm after 4 h incubation, indicating that the drug loaded micelles could be successfully internalized by cancer cells via endocytosis. When the incubation period increased to 12 h and 24 h, the cell uptake of drug loaded micelles was enhanced and the fluorescence became even stronger. Meanwhile, the DOX was mainly located in cytoplasm and partly entered into nuclei for DOX loaded treated cells (Fig. 9B and Fig.9C), suggesting that the DOX had been released and escaped from the endo/lysosomes to the nuclei.

The cellular uptake of DOX loaded micelles was further quantitative evaluated by flow cytometry, and HeLa cells were penetrated with the same process as fluorescence microscopy. As displayed in Fig. 10, the histograms of the pretreated cells incubated with drug loaded micelles shift clearly to the direction of high fluorescence intensity compared with the

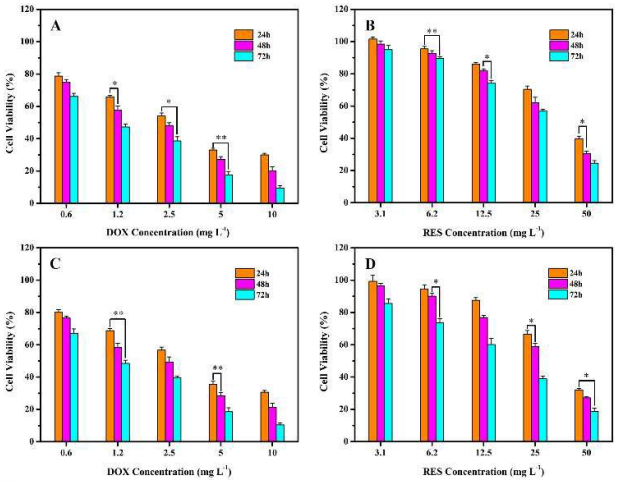

Fig. 8 Cell viabilities of HeLa cells incubated with free DOX (A), free RES (B), DOX-loaded micelles (C), RES-loaded micelles (D) for 24 h, 48 h and 72 h (n = 3, mean ± SD) (*p<0.05, **p<0.01).

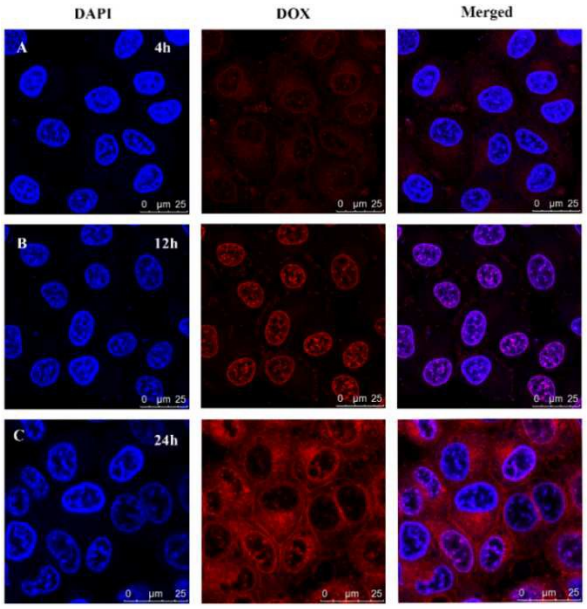

Fig. 9 CLSM images of HeLa cells incubated with DOX loaded micelles after 4 h, 12 h and 24 h.

control cells. Moreover, the mean fluorescence intensity (MFI) of HeLa cells incubated DOX-loaded micelles for 4 h was 10.8, which increased to 21.6 after 24 h incubation, indicating a time-dependent characteristic. These results demonstrated that the stars can efficiently deliver and release drug into tumor cells. The reason might be attributed to different cell uptake pathways of free drugs and drug loaded micelles, and the controlled release manner of drug-loaded micelles.[50]

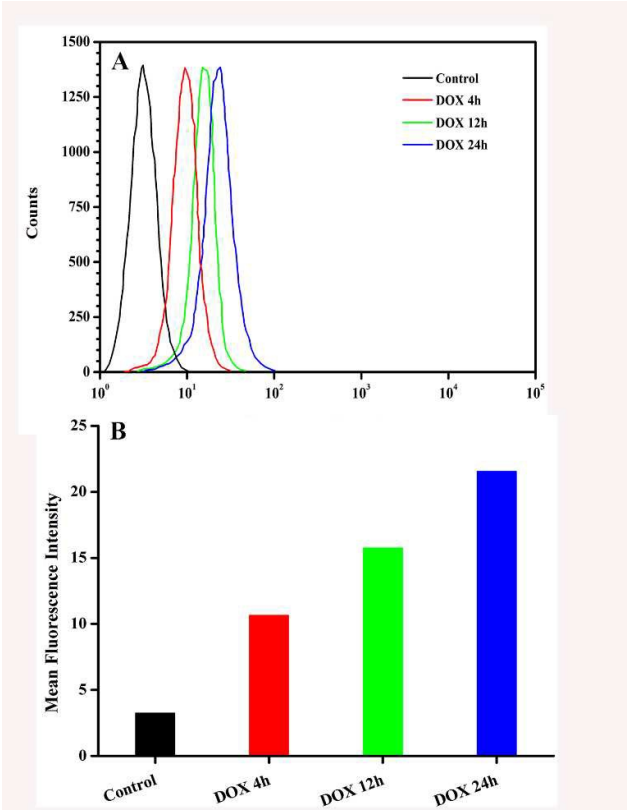

Fig. 10 Flow cytometric profiles and MFI of HeLa cells incubated with DOX loaded micelles for 4h, 12h and 24h.

4. Conclusions

In conclusion, we have successfully synthesized dual responsive core cross-linked star polypeptides based on PLG-P(LP-co-LC) via ring opening polymerization. The micelles self-assembled from the star polypeptides PLG-P(LP-co-LC) have pH and redox sensitivities. DOX and RES were separately loaded into the star polypeptides, and drug loading capacity can be tuned by adjusting the hydrophilic/hydrophobic ratios of the polypeptides. The releases of drugs were accelerated at low pH or high DTT concentration. CLSM images and flow cytometry analysis indicated a fast internalization of the drug loaded micelles *via* endocytosis. The cytotoxicity studies showed that the star polypeptides were non-toxic, and drug loaded micelles exhibited high tumor accumulation and superior antitumor efficiency. It is convinced that these pH and redox-responsive biocompatible micelles have tremendous potential for targeted and controlled intracellular drug delivery.

Acknowledgements

This work was supported by National Key Basic Research Program of China (No.2015CB932100), National "863" Program of China (No.2013AA032201), Program for New Century Excellent Talents in University of China (NCET-12-0760).

Notes and references

1 C. Deng, Y. Jiang, R. Cheng, F. Meng and Z. Zhong, *Nano Today*, 2012, **7**, 467-480.
2 K. Kataoka, A. Harada and Y. Nagasaki, *Adv. Drug Delivery Rev.*, 2012, **64**, 37-48.
3 Z. Ge and S. Liu, *Chem. Soc. Rev.*, 2013, **42**, 7289-7325.
4 Y. Bae and K. Kataoka, *Adv. Drug Delivery Rev.*, 2009, **61**, 768-784.
5 B. Chang, X. Sha, J. Guo, Y. Jiao, C. Wang and W. Yang, *J. Mater. Chem.*, 2011, **21**, 9239-9247.
6 S. P. Nunes, A. R. Behzad, B. Hooghan, R. Sougrat, M. Karunakaran, N. Pradeep, U. Vainio and K. V. Peinemann, *Acs. Nano.*, 2011, **5**, 3516-3522.
7 J. Su, F. Chen, V. L. Cryns and P. B. Messersmith, *J. Am. Chem. Soc.*, 2011, **133**, 11850-11853.
8 D. He, X. He, K. Wang, J. Cao and Y. Zhao, *Langmuir*, 2012, **28**, 4003-4008.
9 H. J. Kim, H. Matsuda, H. Zhou and I. Honma, *Adv. Mater.*, 2006, **18**, 3083-3088.
10 X. Wang, X. Cai, J. Hu, N. Shao, F. Wang, Q. Zhang, J. Xiao and Y. Cheng, *J. Am. Chem. Soc.*, 2013, **135**, 9805-9810.
11 D. L. Liu, X. Chang and C. M. Dong. *Chem. Commun.*, 2013, **49**, 1229-1231.
12 F. Shi, J. Ding, C. Xiao, X. Zhuang, C. He, L. Chen and X. Chen, *J. Mater. Chem.*, 2012, **22**, 14168-14179.
13 T. Zhou, C. Xiao, J. Fan, S. Chen, J. Shen, W. Wu and S. Zhou, *Acta. Biomater.*, 2013, **9**, 4546-4557.
14 H. Deng, Y. Zhang, X. Wang, Y. Cao, J. Liu, J. Liu, L. Deng and A. Dong, *Acta. Biomater.*, 2015, **11**, 126-136.
15 D. J. Phillips, J. P. Patterson, R. K. O'Reilly and M. I. Gibson, *Polym. Chem.*, 2014, **5**, 126-131.
16 S. Yoon, W. J. Kim and H. S. Yoo, *Small*, 2013, **9**, 284-293.
17 K. Liang, G. K. Such, Z. Zhu, Y. Yan, H. Lomas and F. Caruso, *Adv. Mater.*, 2011, **23**, H273-H277.
18 Y. J. Pan, Y. Y. Chen, D. R. Wang, C. Wei, J. Guo, D. R. Lu, C. C. Chu and C.C. Wang, *Biomaterials*, 2012, **33**, 6570-6579.
19 S. C. Owen, D. P. Y. Chan and M. S. Shoichet, *Nano Today*, 2012, **7**, 53-65.
20 F. Meng, R. Cheng, C. Deng and Z. Zhong, *Mater Today*, 2012, **15**, 436-442.
21 G. Kreutzer, C. Ternat, T. Q. Nguyen, C. J. G. Plummer, J. A. E. Manson, V. Castelletto, I. W. Hamley, F. Sun, S. S. Sheiko, A. Herrmann, L. Ouali, H. Sommer, W. Fieber, M. I. Velazco and H. A. Klok, *Macromolecules*, 2006, **39**, 4507-4516.
22 C. Kojima, K. Kono, K. Maruyama and T. Takagishi. *Bioconjugate Chem.*, 2000, **11**, 910-917.
23 J. T. Wiltshire and G. G. Qiao, *Macromolecules*, 2008, **41**, 623-631.
24 B. Helms, S. J. Guillaudeu, Y. Xie, M. McMurdo, C. J. Hawker and J. M. J. Frechet, *Angew. Chem. Int. Ed.*, 2005, **44**, 6384-6387.
25 T. J. Deming, *Prog. Polym. Sci.*, 2007, **32**, 858-875.

26 S. Han, Y. Liu, X. Nie, Q. Xu, F. Jiao, W. Li, Y. Zhao, Y. Wu and C. Chen, *Small*, 2012, **8**, 1596-1606.
27 H. Wu, L. Zhu and V. P. Torchilin, *Biomaterials*, 2013, **34**, 1213-1222.
28 V. K. Kotharangannagari, A. Sanchez-Ferrer, J. Ruokolainen and R. Mezzenga, *Macromolecules*, 2011, **44**, 4569-4573.
29 Y. Xiao, H. Hong, A. Javadi, J. W. Engle, W. Xu, Y. Yang, Y. Zhang, T. E. Barnhart, W. Cai and S. Gong, *Biomaterials*, 2012, **33**, 3071-3082.
30 S. J. Lee, K. H. Min, H. J. Lee, A. N. Koo, H. P. Rim, B. J. Jeon, S. Y. Jeong, J. S. Heo and S. C. Lee, *Biomacromolecules*, 2011, **12**, 1224-1233.
31 W. Chen, P. Zhong, F. Meng, R. Cheng, C. Deng and Z. Zhong, *J. Control. Release.*, 2013, **169**, 171-179.
32 S. Aryal, J. Hu and L. Zhang, *Acs. Nano.*, 2010, **4**, 251-258.
33 J. Dai, S. Lin, D. Cheng, S. Zou and X. Shuai, *Angew. Chem. Int. Ed.*, 2011, **50**, 9404-9408.
34 M. Lagouge, C. Argmann, G. Zachary, H. Meziane, C. Lerin, F. Daussin, N. Messadeq, J. Milne, P. Lambert, P. Elliott, B. Geny, M. Laakso, P. Puigserver and J. Auwerx, *Cell*, 2006, **127**, 1109-1122.
35 J. Zhang, Q. Mi and M. Shen, *Food. Chem.*, 2012, **131**, 879–884.
36 T. Shen, X. N. Wang and H. X. Lou, *Nat. Prod. Rep.*, 2009, **26**, 916-935.
37 A. Mattarei, M. Azzolini, M. Carraro, N. Sassi, M. Zoratti, C. Paradisi and L. Biasutto, *Mol. Pharmaceutics.*, 2013, **10**, 2781-2792.
38 Q. S. Tang, G. W. Li, X. N. Wei, J. Zhang, J. F. Chiu, D. Hasenmayer, D. Z. Zhang and H. Zhang, *Cancer Lett.*, 2013, **336**, 325-337.
39 E. R. Blout and R. H. Karlson, *J. Am. Chem. Soc.*, 1956, **78**, 941-946.
40 C. Gravel, D. Lapierre, J. Labelle and J. W. Keillor, *Can. J. Chem.*, 2007, **85**, 164-174.
41 H. Lu and J. Cheng, *J. Am. Chem. Soc.*, 2007, **129**, 14114-14115.
42 H. Lu and J. Cheng, *J. Am. Chem. Soc.*, 2008, **130**, 12562-12563.
43 M. H. Xiong , J. Wu, Y. C. Wang, L. S. Li, X. B. Liu, G. Z. Zhang, L. F. Yan and J. Wang, *Macromolecules*, 2009, **42**, 893-896.
44 J. T. Wiltshire and G. G. Qiao, *Macromolecules*, 2006, **39**, 4282-4285.
45 S. Takae, K. Miyata, M. Oba, T. Ishii, N. Nishiyama, K. Itaka, Y. Yamasaki, H. Koyama and K. Kataoka, *J. Am. Chem. Soc.*, 2008, **130**, 6001-6009.
46 Y. Tian, L. Bromberg, S. N. Lin, T. A. Hatton and K. C. Tam, *J. Control. Release.*, 2007, **121**, 137-145.
47 M. K. Yu, Y. Y. Jeong, J. Park, S. Park , J. W. Kim, J. J. Min, K. Kim and S. Jon, *Angew. Chem. Int. Ed.*, 2008, **47**, 5362-5365.
48 M. Li, W. Song, Z. Tang, S. Lv, L. Lin, H. Sun, Q. Li, Y. Yang, H. Hong and X. Chen, *Acs. Appl. Mater. Interfaces.*, 2013, **5**, 1781-1792.
49 Z. L. Tyrrell, Y. Shen, and M. Radosz, *Prog. Polym. Sci.*, 2010, **35**, 1128-1143.
50 M. Prabaharan, J. J. Grailer, S. Pilla, D. A. Steeber and S. Gong, *Biomaterials*, 2009, **30**, 5757-5766.

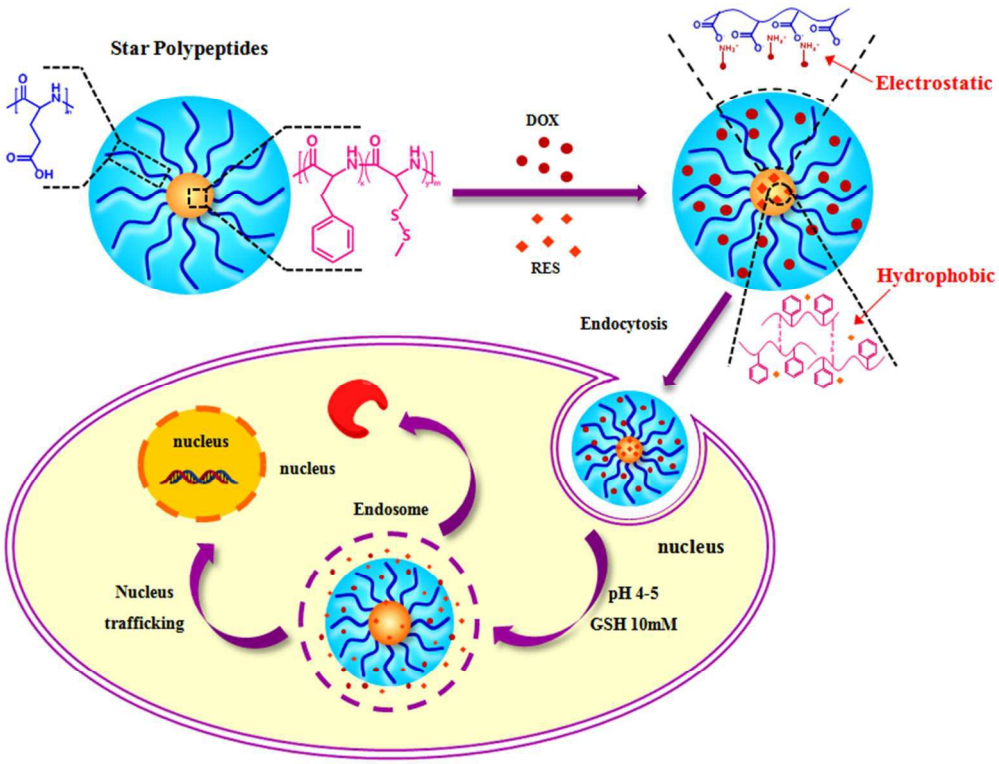

69x52mm (300 x 300 DPI)